Inorganica Chimica Acta 363 (2010) 567–573

Contents lists available at ScienceDirect

Inorganica Chimica Acta

journal homepage: www.elsevier.com/locate/ica

Cyclometalated ruthenium(II) complexes of benzo[*h*]quinoline (bzqH)$[Ru(bzq)(NCMe)_4]^+$, $[Ru(bzq)(LL)(NCMe)_2]^+$, and $[Ru(bzq)(LL)_2]^+$ (LL = bpy, phen)

Ronan Le Lagadec [a,*], Hebert Estevez [a], Ricardo Cerón-Camacho [a], Larissa Alexandrova [b], Alexander D. Ryabov [c,*]

[a] Instituto de Química, Universidad Nacional Autónoma de México, Circuito Exterior s/n, Ciudad Universitaria, 04510 México D.F., Mexico
[b] Instituto de Investigaciones en Materiales, Universidad Nacional Autónoma de México, Circuito Exterior s/n, Ciudad Universitaria, 04510 México D.F., Mexico
[c] Department of Chemistry, Carnegie Mellon University, 4400 Fifth Avenue, Pittsburgh, PA 15213, USA

ARTICLE INFO

Article history:
Received 5 December 2008
Received in revised form 26 February 2009
Accepted 1 March 2009
Available online 13 March 2009

Dedicated to Paul S. Pregosin.

Keywords:
Ruthenium
Cyclometalation
Electrochemistry
Electron transfer
Photosolvolysis

ABSTRACT

Cyclometalation of benzo[*h*]quinoline (bzqH) by $[RuCl(\mu\text{-}Cl)(\eta^6\text{-}C_6H_6)]_2$ in acetonitrile occurs in a similar way to that of 2-phenylpyridine (phpyH) to afford $[Ru(bzq)(MeCN)_4]PF_6$ (**3**) in 52% yield. The properties of **3** containing 'non-flexible' benzo[*h*]quinoline were compared with the corresponding $[Ru(phpy)(MeCN)_4]PF_6$ (**1**) complex with 'flexible' 2-phenylpyridine. The $[Ru(phpy)(MeCN)_4]PF_6$ complex is known to react in MeCN solvent with 'non-flexible' diimine 1,10-phenanthroline to form $[Ru(phpy)(phen)(MeCN)_2]PF_6$, being unreactive toward 'flexible' 2,2′-bipyridine under the same conditions. In contrast, complex **3** reacts both with phen and bpy in MeCN to form $[Ru(bzq)(LL)(MeCN)_2]PF_6$ {LL = bpy (**4**) and phen (**5**)}. Similar reaction of **3** in methanol results in the substitution of all four MeCN ligands to form $[Ru(bzq)(LL)_2]PF_6$ {LL = bpy (**6**) and phen (**7**)}. Photosolvolysis of **4** and **5** in MeOH occurs similarly to afford $[Ru(bzq)(LL)(MeCN)(MeOH)]PF_6$ as a major product. This contrasts with the behavior of $[Ru(phpy)(LL)(MeCN)_2]PF_6$, which lose one and two MeCN ligands for LL = bpy and phen, respectively. The results reported demonstrate a profound sensitivity of properties of octahedral compounds to the flexibility of cyclometalated ligand. Analogous to the 2-phenylpyridine counterparts, compounds **4**–**7** are involved in the electron exchange with reduced active site of glucose oxidase from *Aspergillus niger*. Structure of complexes **4** and **6** was confirmed by X-ray crystallography.

1. Introduction

Cyclometalated ruthenium and osmium complexes have a diverse spectrum of challenging chemical and biochemical properties and potential applications. They are involved in a rapid electron exchange with the active sites of various oxidoreductases and mediate the electron transfer between the enzymes and an electrode [1–6]. Among intriguing chemical features of the ortho-metalated ruthenium derivative of 2-phenylpyridine **1** is a remarkably different reactivity toward two structurally similar bidentate diimine ligands, *viz.* 2,2′-bipyridine and 1,10-phenanthroline (Scheme 1). The ligand substitution reaction between yellow compound **1** with phen cleanly affords brownish compound $\mathbf{2}_{phen}$ in acetonitrile, whereas the bpy ligand just changes the color of **1** into brownish-red without any ligand replacement under identical conditions [4,7]. Photochemical properties of $\mathbf{2}_{phen}$ and $\mathbf{2}_{bpy}$ are also different. Irradiation of $\mathbf{2}_{phen}$ and $\mathbf{2}_{bpy}$ in methanol at room temperature causes photosolvolysis of two and one MeCN ligands, respectively [4]. However, physico-chemical properties of 2,2′-bipyridine and 1,10-phenanthroline are very close and the reasons for such different chemistries, particularly for compound **1**, are still unclear and as such need to be studied more deeply. The major structural dissimilarity of 2,2′-bipyridine and 1,10-phenanthroline is their in-plane rigidity. Nitrogens of bpy have a higher mobility due to a rotation of the pyridine rings around the C–C bond. This is prohibited for phen. The mobility of the *C* and *N* donor centers of *o*-2-phenylpyridinato ligand is obviously similar to that of bpy. Thus, the chemistries described previously [1,4,5] involved combinations of ligands *CN*-flexible–*NN*-flexible and *CN*-flexible–*NN*-nonflexible, orthoruthenated *o*-2-phenylpyridinato being always a flexible partner. In order to verify this flexibility hypothesis, we were intrigued to see the properties of the structurally similar orthoruthenated compounds with the "inverse" structural motives, *viz.* with *CN*-nonflexible–*NN*-flexible and *CN*-nonflexible–*NN*-nonflexible structural combinations.

Therefore we decided to prepare a new ruthenacyclic motif with a rigid and planar benzoquinolate fragment (Scheme 1, bottom).

* Corresponding authors. Tel.: +52 5556224515; fax: +52 5556162203 (R. Le Lagadec).
E-mail addresses: ronan@servidor.unam.mx, lelagadec@gmail.com (R. Le Lagadec).

0020-1693/$ - see front matter © 2009 Elsevier B.V. All rights reserved.
doi:10.1016/j.ica.2009.03.006

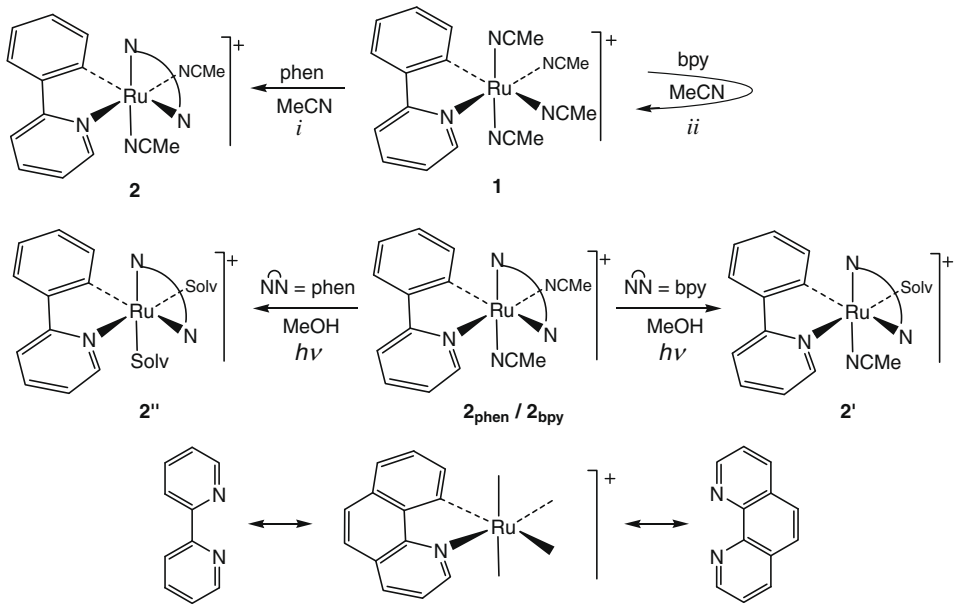

Scheme 1. Unusual properties of cycloruthenated complexes **1** and **2** [4] and cycloruthenated skeleton of benzo[*h*]quinoline (bottom) investigated in this work. See text for details.

Benzo[*h*]quinoline (bzqH) is known to form readily orthometalated complexes with various transition metals. The first preparation of palladium(II) complexes was reported in 1969 by Nonoyama et al. [8]. Ruthenium derivatives are however less common. The first complex described was the bis-metalacycle $[Ru(bzq)_2(CO)_2]$ [9], the CO ligands of which were later photosubstituted by pyridine or PPh_3 [10]. Mono-cyclometalated species $[RuCl(bzq)L_3]$ (L = CO, PPh_3) were described by Hiraki et al. [11]. The complex $[RuH(H_2)(bzq)(P^iPr_3)_2]$ was prepared from [Ru(COD)(COT)] (COD = 1,5-C_8H_{12}; COT = 1,3,5-C_8H_{10}) for studying hydrogen exchange processes [12]. An easy preparation of the neutral compound $[RuCl(\eta^6\text{-}C_6H_6)(bzq)]$ from $[RuCl(\mu\text{-}Cl)(\eta^6\text{-}C_6H_6)]_2$ and bzqH in methanol was reported very recently [13]. Related to our work, the complex $[Ru(bzq)(bpy)_2]PF_6$ (**6**) was first prepared by Reveco et al., from $[Ru(bpy)_2(MeOCH_2CH_2OMe)](PF_6)_2$ and bzqH, but the yield was just 8% [14]. In this paper, we describe a facile high-yield preparation of a series of ruthenium(II) complexes of benzo[*h*]quinoline and their physico-chemical properties including their activity as mediators in the electron exchange with glucose oxidase (GO).

2. Experimental

2.1. Syntheses

All experiments were performed under dry argon using Schlenk techniques. All solvents were dried and distilled under nitrogen prior to use. *N*,*N*-dimethylbenzylamine, 2-phenylpyridine, potassium hexafluorophosphate, tetra-*n*-butylammonium hexafluorophosphate, 2,2′-bipyridine, 1,10-phenanthroline, 1,3-cyclohexadiene, glucose oxidase from *Aspergillus niger* (type VII) were purchased from Sigma Aldrich Chemical and were used as received. Ruthenium trichloride was purchased from Strem Chemicals and converted into $[RuCl(\mu\text{-}Cl)(\eta^6\text{-}C_6H_6)]_2$ as described elsewhere [15]. The activity of glucose oxidase in terms of catalytically active FAD was determined spectrophotometrically using the extinction coefficient of $1.31 \times 10^4\ M^{-1}\ m^{-1}$ at 450 nm [16].

2.1.1. $[Ru(bzq)(NCMe)_4]PF_6$ (**3**)

To a suspension of $[RuCl(\mu\text{-}Cl)(\eta^6\text{-}C_6H_6)]_2$ (500 mg, 1.00 mmol), KPF_6 (736 mg, 4.00 mmol) and KOH (112 mg, 2.00 mmol) in 50 mL of acetonitrile was added 7,8-benzoquinoline (448 mg, 2.5 mmol). The mixture was heated at 40 °C for 60 h. The solvent was evaporated under vacuum, and the residue was dissolved in 10 mL of CH_2Cl_2. The solution was filtered through Al_2O_3, using first CH_2Cl_2, and then a 5:1 CH_2Cl_2/CH_3CN mixture as eluent. The bright yellow fraction was collected and evaporated to dryness. Crystallization from CH_2Cl_2:CH_3CN(5:1)/diethylether (slow diffusion) gave orange crystals, which were washed with diethylether and dried under vacuum (611 mg, 52%). ^1H NMR (δ, CD_3CN): 9.18 (dd, 1H, ^3J = 5.2 Hz, ^4J = 1.4 Hz), 8.26 (dd, 1H, ^3J = 8.1 Hz, ^4J = 1.35), 8.17 (dd, 1H, ^3J = 5.8 Hz, ^4J = 2.3 Hz), 7.83 (d, 1H, ^3J = 8.8 Hz), 7.67 (d, 1H, ^3J = 8.7 Hz), 7.53 (dd, 1H, ^3J = 8.0 Hz, ^4J = 5.38 Hz), 7.49 (d, 1H, ^3J = 4.0 Hz), 7.48 (s, 1H), 2.58 (s, 3H, $NCCH_3$), 1.96 (s, 3H, $NCCH_3$), 1.90 (s, 6H, $2NCCH_3$). ^{31}P NMR: −144 (hep, PF_6). MS-FAB$^+$: 444 (2%) $[M+H]^+$, 403 (25%) $[M+H-NCCH_3]^+$, 362 (5%) $[M+H-2NCCH_3]^+$, 321 (7%) $[M+H-3NCCH_3]^+$, 280 (4%) $[M+H-4NCCH_3]^+$. IR: 838 (s, PF_6), 2277 (m, $\nu_{N\equiv C}$). *Anal.* Calc. for $C_{21}H_{20}F_6N_5PRu$: C, 42.86; H, 3.43; N, 11.90. Found: C, 41.94; H, 3.48; N, 11.12%.

2.1.2. $[Ru(bzq)(bpy)(NCMe)_2]PF_6$ (**4**)

A solution of **3** (250 mg, 0.43 mmol) with 2,2′-bipyridine (132 mg, 0.85 mmol) in acetonitrile (30 mL) was stirred a room temperature for 48 h. The solvent was evaporated under vacuum, and the dark brown residue was dissolved in 10 mL of CH_2Cl_2. The solution was filtered through Al_2O_3 first using CH_2Cl_2, then a 10:3 CH_2Cl_2/NCMe mixture as eluent. The brown fraction was collected and evaporated to dryness under vacuum. Crystallization from CH_2Cl_2:CH_3CN (3:1)/diethylether (slow diffusion) gave dark brown crystals, which were washed with diethylether and dried under vacuum (171 mg, 60%). ^1H NMR (δ, CD_3CN): 9.47 (ddd, 1H, ^3J = 5.5 Hz, ^4J = 1.7 Hz, ^4J = 0.8 Hz), 8.48 (dt, 1H, ^3J = 8.0 Hz, ^4J = 1.1 Hz,), 8.44 (dd, 1H, ^3J = 6.9 Hz, ^4J = 1.1 Hz), 8.21 (td, 1H, ^3J = 7.7 Hz, ^4J = 0.5 Hz), 8.21 (dt, 1H, ^3J = 8.0 Hz, ^4J = 1.11 Hz), 8.05 (dd, 1H, ^3J = 8.0 Hz, ^4J = 1.4 Hz,), 7.91-7.86 (m, 2H), 7.74 (ddd,1H, ^3J = 5.8, Hz, ^4J = 1.7 Hz, ^4J = 0.8 Hz), 7.71-7.57 (m, 5H), 7.11 (dd, 1H, ^3J = 8.2 Hz, ^4J = 5.5 Hz), 6.84 (ddd, 1H, ^3J = 7.4, ^3J = 5.8 Hz, ^4J = 1.4), 2.25 (s, 3H, $NCCH_3$,), 2.12 (s, 3H, $NCCH_3$). ^{31}P NMR: −143.99 (hep, PF_6). MS-FAB$^+$: 663 (4%) $[M+H+PF_6]^+$, 517 (22%) $[M+H]^+$, 477 (19%) $[M+H-NCCH_3]^+$, 435 (72%) $[M+H-2NCCH_3]^+$, 279 (10%) $[M+H-2NCCH_3-bpy]^+$, 257 (7%) $[M+H-2NCCH_3-bzq]^+$.

IR: 843 (s, PF_6), 2267 (m, $\nu_{N\equiv C}$). *Anal.* Calc. for $C_{27}H_{22}F_6N_5PRu$: C, 48.95; H, 3.35; N, 10.57. Found: C, 48.59; H, 3.35; N, 9.94%.

2.1.3. [Ru(bzq)(phen)(NCMe)$_2$]PF$_6$ (**5**)

Compound **5** was obtained under the same conditions as **4** from **3** (250 mg, 0.43 mmol) and 1,10-phenanthroline (190 mg, 1.06 mmol) in 57% yield (168 mg).

^{1}H NMR (δ, CD_3CN): 9.81 (d, 1H, ^3J = 4.9), 8.75 (d, 1H, ^3J = 8.3), 8.52 (d, 1H, ^3J = 6.9), 8.25–8.13 (m, 3H), 8.02–7.97 (m, 3H), 7.91 (d, 1H, ^3J = 8.8 Hz), 7.72 (t, 1H, ^3J = 7.2 Hz), 7.64–7.57 (m, 3H), 7.2 (dd, 1H, ^3J = 8.0, ^3J = 5.5), 6.95 (dd, 1H, ^3J = 7.3 Hz ^3J = 5.5 Hz), 2.19 (s, 3H, $NCCH_3$), 2.14 (s, 3H, $NCCH_3$). ^{31}P NMR: −144(hep, PF_6). MS-FAB$^+$: 687 (3%) [M+H+PF_6]$^+$, 542 (11%) [M+H]$^+$, 501 (7%) [M+H−$NCCH_3$]$^+$, 460 (29%) [M+H−2$NCCH_3$]$^+$, 280 (7%) [M+H−2$NCCH_3$−phen]$^+$. IR: 842 (s, PF_6), 2267 (m, $\nu_{N\equiv C}$). *Anal.* Calc. for $C_{29}H_{22}F_6N_5PRu \cdot 0.5CH_2Cl_2$: C, 48.60; H, 3.18; N, 9.61. Found: C, 48.61; H, 3.37; N, 10.03%.

2.1.4. [Ru(Bzq)(bpy)$_2$]PF$_6$ (**6**)

A solution of **3** (250 mg, 0.43 mmol) with 2,2′-bipyridine (200 mg, 1.28 mmol) in methanol (40 mL) was heated at 45 °C for 20 h. The solvent was evaporated under vacuum, and the dark brown residue was dissolved in 10 mL of CH_2Cl_2. The solution was filtered through Al_2O_3 first using CH_2Cl_2, then a 7:1 CH_2Cl_2/NCMe mixture as eluent. The purple fraction was collected and evaporated to dryness under vacuum. Crystallization from CH_2Cl_2:CH_3CN (7:1)/diethylether (slow diffusion) gave dark purple crystals, which were washed with diethylether and dried under vacuum (175 mg, 55%). ^{1}H NMR (δ, CD_3CN): 8.48 (d, 1H, ^3J = 8.2 Hz), 8.37-8.33 (m, 2H), 8.28 (d, 1H, ^3J = 8.2), 8.19 (dd, 1H, ^3J = 8.0 Hz, ^4J = 1.2 Hz), 8.04–7.98 (m, 2H), 7.88–7.82 (m, 5H), 7.76–7.67 (m, 3H), 7.62 (dd, 1H, ^3J = 5.8 Hz, ^4J = 0.5 Hz), 7.48–7.40 (m, 2H), 7.32–7.21 (m, 3H), 7.05–6.98 (m, 2H), 6.68 (d, 1H, ^3J = 6.9 Hz), ^{31}P NMR: −144(hep, PF_6). MS-FAB$^+$: 737 (3%) [M+H+PF_6]$^+$, 592 (78%) [M+H]$^+$, 436 (28%) [M+H−bpy]$^+$, 280 (4%) [M+H−2bpy]$^+$. IR: 842 (s, PF_6). *Anal.* Calc. for $C_{33}H_{24}F_6N_5PRu \cdot 0.5CH_2Cl_2$: C, 51.65; H, 3.23; N, 8.99. Found: C, 51.29; H, 3.31; N, 8.63%.

2.1.5. [Ru(Bzq)(phen)$_2$]PF$_6$ (**7**)

Compound **7** was obtained under the same conditions as **6** from **3** (250 mg, 0.43 mmol) and 1,10-phenanthroline (230 mg, 1.28 mmol) in 51% yield (172 mg). ^{1}H NMR (δ, CD_3CN) 8.76 (d, 1H, ^3J = 8.3 Hz), 8.64 (d, 1H, ^3J = 7.4 Hz), 8.60 (d, 1H, ^3J = 8.0 Hz), 8.54 (d, 1H, ^3J = 8.0 Hz), 8.29 (dd, 1H, ^3J = 8.0 Hz, ^4J = 1.1 Hz) 8.18–8.12 (m, 2H), 8.04–7.75 (m, 9H), 7.62 (ddd, 1H, ^3J = 7.4, ^3J = 5.5, ^4J = 1.1), 7.44–7.38 (m, 3H), 7.27–7.15 (m, 3H), 6.75 (d, 1H, ^3J = 6.9 Hz). ^{31}P NMR: −144 (hep, PF_6). MS-FAB$^+$: 640 (2%) [M+H]$^+$, 460 (29%) [M+H−phen]$^+$, 280 (4%) [M+H−2phen]$^+$. IR: 842 (s, PF_6). *Anal.* Calc. for $C_{37}H_{24}F_6N_5PRu$: C, 56.64; H, 3.08; N, 8.93. Found: C, 55.84; H, 3.58; N, 8.49%.

2.2. Physical measurements

All NMR spectra were recorded on a JEOL GX300 (^{1}H at 300.53 MHz) spectrometer in CD_3CN. Chemical shits (δ, ppm) are referenced to the residual solvent peaks. Coupling constants (J) are in Hz. Mass spectra (FAB$^+$) were obtained using a JEOL JMS-SX102A instrument with *m*-nitrobenzyl alcohol as a matrix. IR spectra were recorded on a Bruker-Tensor 27 FT-IR apparatus (KBr disks, diffuse reflection mode). Elemental analyses were carried out by USAI-UNAM on an EA 1108 FISONS Instrument analyzer. Electrochemical measurements were performed on a PC-interfaced potentiostat–galvanostat AUTOLAB PGSTAT 12. A three-electrode setup was used with a BAS working glassy carbon electrode, Ag/AgCl reference electrode, and auxiliary Pt electrode. Before each measurement, the working electrode was polished with a diamond paste and rinsed with acetone and distilled water. Anodic peak currents (i_o) were obtained from cyclic voltammograms

Table 1
Crystallographic data for compounds **4** and **6**.

	4 · CH_2Cl_2	**6** · 0.5CH_2Cl_2
Empirical formula	$C_{27}H_{22}F_6N_5PRu \cdot CH_2Cl_2$	$C_{66}H_{48}F_{12}N_6P_2Ru_2 \cdot CH_2Cl_2$
Formula weight	747.46	1558.15
T (K)	291(2)	291(2)
Crystal system	monoclinic	monoclinic
Wavelength (Å)	0.71073	0.71073
Space group	$P2_1/c$	$P2_1/c$
Unit cell dimensions		
a (Å)	15.2255(12)	24.0282(16)
b (Å)	13.7004(11)	14.0507(9)
c (Å)	16.1399(12)	19.3602(13)
α (°)	90	90
β (°)	114.4180(10)	104.547(2)
γ (°)	90	90
V (Å^3)	3065.6(4)	6326.7(7)
Z	4	4
Density (mg/m^3, calculated)	1.620	1.636
Absorption coefficient (mm^{-1})	0.802	0.700
F(000)	1496	3128
Crystal size (mm)	0.28 × 0.18 × 0.18	0.36 × 0.18 × 0.04
θ range for data collection (°)	2.03–25.35	1.69–25.34
Index ranges	$-18 \leqslant h \leqslant 18$	$-28 \leqslant h \leqslant 28$
	$-16 \leqslant k \leqslant 16$	$-16 \leqslant k \leqslant 16$
	$-19 \leqslant l \leqslant 19$	$-23 \leqslant l \leqslant 23$
Reflections collected	25388	52325
Independent reflections [$R_{(int)}$]	5625 [0.0434]	11555 [0.1198]
Absorption correction	empirical	empirical
Refinement method	full-matrix least-squares on F^2	full-matrix least-squares on F^2
Data/restraints/parameters	5625/1045/629	11555/888/991
Goodness-of-fit (GOF) on F^2	0.960	0.812
Final R indices [$I > 2\sigma$(I)]	R_1 = 0.0451, wR_2 = 0.1110	R_1 = 0.0587, wR_2 = 0.0954
R indices (all data)	R_1 = 0.0609, wR_2 = 0.1165	R_1 = 0.1512, wR_2 = 0.1099
Largest difference peak and hole (e Å^{-3})	0.879 and −0.470 0	595 and −0.598

in the absence of the enzyme. Catalytic currents (i_{cat}) were obtained in the presence of GO and D-glucose under nitrogen. The rate constants, k_3, were calculated from the slopes of linear plots of the ratio i_{cat}/i_o against $([GO]/v)^{1/2}$ (v is the scan rate), as originally described elsewhere [17] and applied in our previous studies [1–3,6,18]. Solutions of photolabile acetonitrile ruthenium complexes were irradiated using a Cole-Parmer Standard Fiber Optic Illuminator fitted with a 150 W halogen lamp.

2.3. X-ray crystallography

Diffraction intensities data were collected with a SMART APEX diffractometer equipped with a graphite monochromated Mo Kα radiation and CCD area detector at room temperature. The detector was placed at a distance of 4.837 cm from the crystals in all cases. A total of 1800 frames were collected with a scan width of 0.3 in ω and an exposure time of 10 s/frame. The frames were integrated with the Bruker SAINT software package [19] using a narrow-frame integration algorithm. The intensity data were corrected by Lorentz and polarization effects and analytical absorption correction was applied in all cases. The data integration was done using a monoclinic unit cell for **4** and **6** to yield a total of 25388 and 52325 reflections, respectively, of which 5625 to **4** and 11555 to **6** were independent. Analysis of the data showed negligible decay during the data collection in all cases. The structures were solved by Patterson method using SHELXS-97 [20] program and completed by subsequent difference Fourier synthesis map and refined by full matrix least-squares procedures on F^2. Hydrogen atoms were input at calculated positions, and allowed to ride on the atoms to which they are attached. For all complexes, the final cycle of refinement was carried out on all non-zero data using SHELXL-97 and anisotropic thermal parameters for all non-hydrogen atoms. The structures have incorporated solvent molecules, which were refined isotropically. The distorted anions PF_6^- in all crystal structures were modeled and refined anisotropically in two major contributors. All calculations were performed using the SHELXTL (6.12) program package. Additional details are summarized in Table 1.

3. Results and discussion

3.1. Synthesis

Complex **3**, $[Ru(bzq)(NCMe)_4]PF_6$, was prepared using the method developed for the cyclometalation of 2-phenylpyridine and *N*,*N*-dimethylbenzylamine (Scheme 2). The dimer $[RuCl(\mu\text{-}Cl)(\eta^6\text{-}C_6H_6)]_2$ was reacted with benzo[*h*]quinoline in acetonitrile in the presence of a base [21]. The yellow crystalline compound formed is stable under inert atmosphere, but decomposes readily into a greenish material if exposed to air. It is important to note that in this case, as observed for 2-phenylpyridine, but not for *N*,*N*-dimethylbenzylamine and analogous osmium derivatives, the substitution of η^6-benzene by MeCN takes place under the reaction conditions. Another important feature is that the metalation of benzo[*h*]quinoline needs longer time than for the metalation of 2-phenylpyridine, *viz.* 60 *versus* 20 h, to achieve a reasonable yield of 52%. This observation is in qualitative agreement with the previously proposed electrophilic mechanism of sp^2 C–H bond cyclometalation of 2-phenylpyridine by $[RuCl(\mu\text{-}Cl)(\eta^6\text{-}C_6H_6)]_2$ [21]. In fact, in their earlier work Dewar and Warford introduced the reactivity factors that show a relative tendency of a particular sp^2 C–H bond of arene to undergo electrophilic substitution irrespective of electrophilic agent used [22]. Their estimates predict that the reactivity factors for position 2 of biphenyl and 4 of phenanthrene equal 2.07 and 1.96, respectively (Scheme 3, X = CH). Provided similar trend holds for X = N, 2-phenylpyridine should undergo faster electrophilic cyclometalation than benzo[*h*]quinoline. There is no conflict with a common belief that benzo[*h*]quinoline is easy to cyclometalate [9,23,24]. It should only be taken into account that "ready metalation" is not synonym for "faster rate". Non-flexible quinoline unit with C–H containing groups at position 8 are directed at a metal center if the ligand is coordinated via its nitrogen atom. Thus, the spatial correspondence is created between the C–H bond and a metal center favorable for the C–H activation [25]. This phenomenon was previously analyzed by Pregosin and co-workers [26,27].

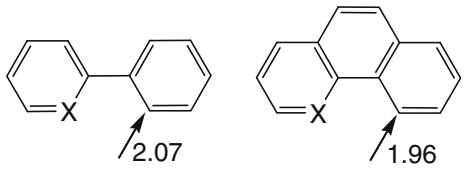

Scheme 3. Reactivity numbers for position position 2 of biphenyl and 4 of phenanthrene (X = CH). See text for details.

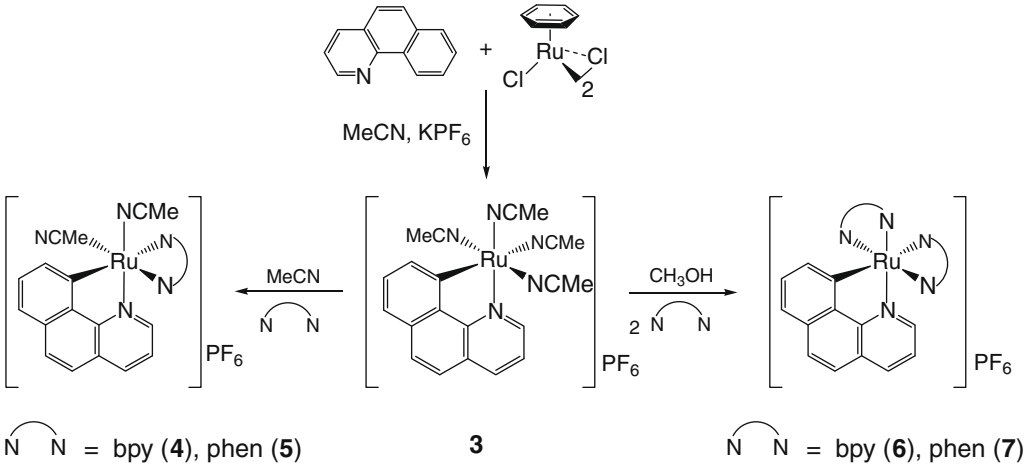

Scheme 2. Synthetic procedures used in this work.

Air-stable, deep purple complexes **4**–**7** were obtained from **3** in 50–60% yield on prolonged treatment with bpy or phen in MeCN (48 h, **4** and **5**) or MeOH (20 h, **6** and **7**) (Scheme 2). Analytically pure compounds were obtained after recrystallization and all complexes were fully characterized by elemental analysis, ^{1}H NMR, MS and cyclic voltammetry. Interestingly, contrary to the reactivity of **2**, no difference was observed when **3** was reacted with bpy or phen in acetonitrile. In both cases, the bis-acetonitrile ruthenium(II) complexes were obtained in around 60% yield. Therefore, the non-flexible cycloruthenated ligand rules out the different reactivity of **3** toward bpy and phen in MeCN solvent by assisting flexible bpy in entering the coordination sphere of Ru^{II}. A tentative assistance mechanism could be stacking/hydrophobic in origin. We propose that bpy may interact with the plane of cyclometalated benzo[*h*]quinoline more productively than with that of 2-phenylpyridine. The interaction flattens the bpy ligand and brings its nitrogens into the ligand plane. Such a conformer of bpy could be the optimal for chelation due to kinetic reasons, the reactivity of bpy may increase, and this may account for the observation of similar reactivity of bpy and phen with respect to substitution of MeCN ligands in **3**.

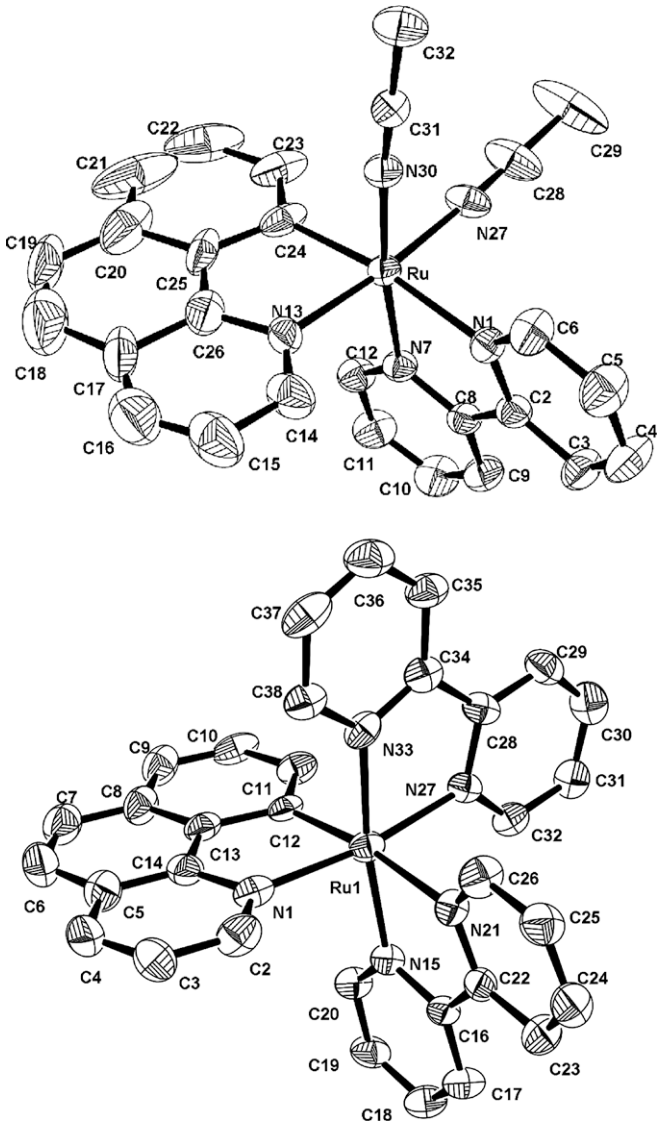

Fig. 1. ORTEP views of ruthenacycles **4** and **6**. Thermal ellipsoids are drawn with 50% probability level. Hydrogen atoms and PF_6^- anions are omitted for clarity.

3.2. X-ray structural studies

Crystals suitable for X-ray diffraction studies were obtained for compounds **4** and **6** (Fig. 1). Selected bond distances and angles are collected in Table 2. The ruthenium atom is in the center of a slightly distorted octahedron for **4** and **6**. As observed for similar compounds, the 2 MeCN ligands in **4** are coordinated *cis* to each other [1,3]. As before, the Ru–N bonds in *trans* position to the σ-bound carbon atom are elongated in comparison to the other Ru–N bonds [1,3] due to a strong *trans* influence of the carbon atom.

3.3. Cyclic voltammetry

Complexes **3**–**7** showed a reversible one electron wave for the Ru^{II}/Ru^{III} transition in acetonitrile in the 540–740 mV range (*versus* Ag/AgCl). In water containing about 5% acetonitrile for increasing solubility, the potentials are by 200–300 mV lower, although the reversibility is not as good as in acetonitrile. The electrochemical data are summarized in Table 3. Compounds **6** and **7** with two diimine bidentate ligands have slightly lower reduction potentials than **4** and **5** with 2 MeCN ligands. This is probably due to a stronger back-bonding capability of acetonitrile in comparison to bpy or phen. When compared to the related compounds in which the cyclometalated fragment is phpy the reduction potentials are slightly higher for **4**–**7** in acetonitrile but are slightly lower in water [1,4,6]. The difference is of *ca.* 20 mV; it is not large enough to attribute it to different electronic effects of cycloruthenated 2-phenylpyridine and benzo[*h*]quinoline.

3.4. Photosolvolysis of acetonitrile ligands of *4* and *5*

Cyclometalated benzo[*h*]quinoline, in contrast to 2-phenylpyridine, minimizes dissimilarity of complexes **4** and **5**. Their cyclic

Table 2
Selected bond distances (Å) and angles (°) for compounds **4** and **6**.

4		**6**	
Ru–N(30)	2.014(4)	Ru(1)–N(33)	2.050(6)
Ru–N(27)	2.018(4)	Ru(1)–N(27)	2.050(5)
Ru–N(7)	2.052(3)	Ru(1)–N(15)	2.062(5)
Ru–N(13)	2.077(4)	Ru(1)–N(1)	2.088(6)
Ru–N(1)	2.135(3)	Ru(1)–N(21)	2.134(5)
Ru–C(24)	2.036(5)	Ru(1)–C(12)	2.041(7)
N(30)–Ru–N(27)	86.37(13)	N(33)–Ru(1)–N(27)	78.3(3)
N(27)–Ru–N(7)	90.82(13)	N(27)–Ru(1)–N(15)	96.8(2)
N(30)–Ru–N(13)	89.6(3)	N(33)–Ru(1)–N(1)	94.8(2)
N(7)–Ru–N(13)	94.3(3)	N(15)–Ru(1)–N(1)	90.5(2)
N(30)–Ru–C(24)	90.2(4)	N(33)–Ru(1)–C(12)	90.5(2)
N(27)–Ru–C(24)	97.9(2)	N(27)–Ru(1)–C(12)	95.0(3)
N(7)–Ru–C(24)	96.9(4)	N(15)–Ru(1)–C(12)	95.7(2)
N(13)–Ru–C(24)	81.7(3)	N(1)–Ru(1)–C(12)	80.0(3)
N(30)–Ru–N(1)	95.70(13)	N(33)–Ru(1)–N(21)	96.8(2)
N(27)–Ru–N(1)	91.77(17)	N(27)–Ru(1)–N(21)	90.35(19)
N(7)–Ru–N(1)	77.60(13)	N(15)–Ru(1)–N(21)	77.3(2)
N(13)–Ru–N(1)	91.23(17)	N(1)–Ru(1)–N(21)	95.4(2)

Table 3
Reduction potentials (in mV *vs.* Ag/AgCl) at 25 °C, scan rate 0.1 V s^{-1}, 0.1 M (*n*-Bu)$_4$NPF$_6$ in CH_3CN or water (containing *approx.* 5% CH_3CN for increasing solubility) and the rate constants k_3 (in M^{-1} s^{-1}) for oxidation of GO (red) by the electrochemically generated Ru^{III} species at pH 7.0 (0.01 M phosphate).

Compound	MeCN	H_2O	$10^6 \times k_3$
[Ru(bzq)(NCMe)$_4$]PF$_6$ (**3**)	743	405	[a]
[Ru(bzq)(bpy)(NCMe)$_2$]PF$_6$ (**4**)	630	379	7 ± 2
[Ru(bqz)(phen)(NCMe)$_2$]PF$_6$ (**5**)	625	408	1.5 ± 0.2
[Ru(bzq)(bpy)$_2$]PF$_6$ (**6**)	546	307	7.4 ± 0.6
[Ru(bzq)(phen)$_2$]PF$_6$ (**7**)	544	301	6 ± 2

[a] Was not measured.

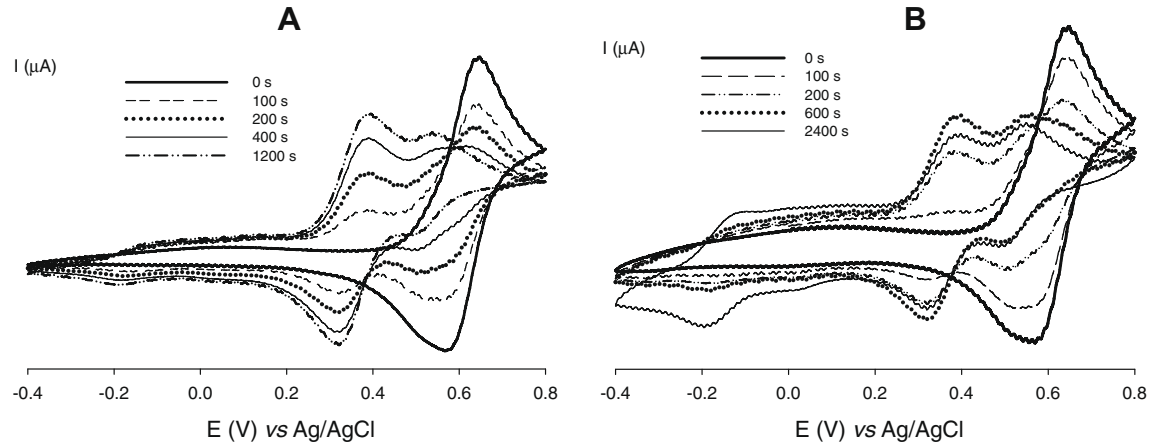

Fig. 2. Cyclic voltammograms of complexes **4** (A) and **5** (B) in MeOH obtained before (0 s) and after irradiation (at different times) by a 150 W halogen lamp. Substraction of the background signal was applied. Conditions: [Ru^{II}] 1×10^{-3} M, [$(n\text{-Bu})_4NPF_6$] 0.1 M, scan rate 100 mV s^{-1}.

voltammograms obtained in MeOH are similar to those in MeCN as solvent. There are reversible waves at 610 and 608 mV for **4** and **5**, respectively (Fig. 2A and B). Irradiation of the solutions by a 150 W halogen lamp brings about similar changes in cyclic voltammograms of **4** and **5**. The Nernstian features at 610 and 608 mV disappear and several new features are observed, the dominating being the quasi-reversible ones seen at 360 and 347 mV, for **4** and **5**, respectively. Thus, the reduction potential of the main wave decreases similarly by ca. 260 mV. This behavior is similar to that of $\mathbf{2}_{bpy}$ but contrasts severely to that of $\mathbf{2}_{phen}$, for which the reduction potential decreased by 800 mV [4]. The changes were accounted by the photosolvolysis of one and two MeCN ligands, respectively. Our quantitative estimation [4] made on the basis of the electrochemical parameterization concept of Lever [28] indicates that the replacement of one MeCN ligand by MeOH should decrease the reduction potential of ruthenium complex by ca. 300 mV. The data shown in Fig. 2A and B agree with the prediction made and are indicative of the fact that the major species formed have just one coordinated methanol molecule. Thus, cycloruthenated nonflexible benzo[*h*]quinoline as opposed to flexible 2-phenylpyridine eliminates dissimilarity of **4** and **5** in the solvolytic photosubstitution.

It should be mentioned that the photosolvolysis of **4** and **5** proceed less cleanly than for the formation of **2′** and **2″** in Scheme 1. A number of other signals are also generated, which may result either from newly generated species or be adsorptive in origin [29]. For example, less intense waves are seen as well at 521, −44 (irreversible), and −185 mV after 10 min of irradiation of **4**. For phen complex **5** these are observed at 527, −44, and −186 mV. A notable reversible wave at −186 mV is more pronounced for **5** than for **4** for the same reaction time, indicating the solvolysis of two MeCN ligands may also take place. But in any case, it is significantly weaker than for the 2-phenylpyridine analogue **2″**. The substitution of both acetonitrile ligands by solvent molecules is much more difficult than that for the 2-phenylpyridine complexes and after 30 min of irradiation only a small amount of the monosubstituted compound (**2′**-like) was converted into the disubstituted one (**2″**-like).

3.5. Electron transfer with glucose oxidase (GO) from Aspergillus niger

As mentioned earlier, cyclometalated octahedral ruthenium(II) complexes structurally similar to **4**–**7** show exceptional activity as electron carriers to/from active sites of oxidoreductases. Those results encouraged us to test our new complexes as mediators of the GO enzyme. Eqs. (1)–(3) show the key reactions of the mediated oxidation of β-D-glucopyranose into the corresponding γ-lactone

$$GO(ox) + D\text{-glucose} \rightarrow GO(red) + \delta\text{-}D\text{-gluconolactone} + 2H^+ \quad (1)$$

$$GO(red) + 2Ru^{III} \xrightarrow{k_3} GO(ox) + 2Ru^{II} \quad (2)$$

$$2Ru^{II} - 2e \rightarrow 2Ru^{III}(electrode) \quad (3)$$

Step 2 is known to follow the second-order kinetics and the corresponding rate constants k_3 for step 2 calculated by means of the procedure of Bourdillon et al. [17] are shown in Table 3. The rate constants k_3 are high for all compounds, and no significant difference was observed between the complexes. The values of k_3 are comparable to the highest values reported for the 2-phenylpyridine complexes and are just slightly lower than 1×10^7 M^{-1} s^{-1} reported for $[Ru(dmba)(bpy)_2]PF_6$ [1,3]. Thus, the flexibility effect in the orthometalated fragment does not seem to play a role in the kinetics of electron exchange with the reduced active site of glucose oxidase from *A. niger*.

4. Conclusion

Ruthena(II)cycles bearing the non-flexible benzo[*h*]quinoline ligand are easy to make and we have prepared several structural analogues of cycloruthenated complexes of flexible 2-phenylpyridine with 2,2′-bipyridine and 1,10-phenanthroline ligands, which are known to have different properties and/or reactivity depending on whether bpy or phen is an additional diimine ligand. None of the differences found for the 2-phenylpyridine complexes is observed for similar derivatives of benzo[*h*]quinoline. Its cycloruthenated derivatives with bpy and phen behave similar. This study suggests that the concept introduced here of flexibility/non-flexibility of cyclometalated and ancillary bidentate ligands is worth further attention as a tool for a fine tuning of properties and reactivity of octahedral cyclometalated compounds. However, the benzo[*h*]quinoline ligand does not compromise the ability of the complexes to serve as electron shuttles between the actives sites of GO and an electrode.

Acknowledgements

We thank PAPIIT and CONACyT for financial support (Projects 205209 and 57556) and for research grants to H.E. and R.C.-C. Simón Hernández is gratefully acknowledged for performing X-ray crystallographic experiments.

Appendix A. Supplementary material

CCDC 721265 and 721266 contain the supplementary crystallographic data for **4** and **6**. These data can be obtained free of charge from The Cambridge Crystallographic Data Centre via www.ccdc.cam.ac.uk/data_request/cif. Supplementary data associated with this article can be found, in the online version, at doi:10.1016/j.ica.2009.03.006.

References

[1] A.D. Ryabov, V.S. Sukharev, L. Alexandrova, R. Le Lagadec, M. Pfeffer, Inorg. Chem. 40 (2001) 6529.
[2] A.D. Ryabov, V.S. Soukharev, L. Alexandrova, R. Le Lagadec, M. Pfeffer, Inorg. Chem. 42 (2003) 6598.
[3] R. Le Lagadec, L. Rubio, L. Alexandrova, R. Toscano, E.V. Ivanova, R. Meškys, V. Laurinavičius, M. Pfeffer, A.D. Ryabov, J. Organomet. Chem. 689 (2004) 4820.
[4] A.D. Ryabov, R. Le Lagadec, H. Estevez, R.A. Toscano, S. Hernandez, L. Alexandrova, V.S. Kurova, A. Fisher, C. Sirlin, M. Pfeffer, Inorg. Chem. 44 (2005) 1626.
[5] R. Le Lagadec, L. Alexandrova, H. Estevez, M. Pfeffer, V. Laurinavièius, J. Razumiene, A.D. Ryabov, Eur. J. Inorg. Chem. (2006) 2735.
[6] R. Cerón-Camacho, D. Morales-Morales, S. Hernández, R. Le Lagadec, A.D. Ryabov, Inorg. Chem. 47 (2008) 4988.
[7] A.D. Ryabov, H. Estevez, L. Alexandrova, M. Pfeffer, R. Le Lagadec, Inorg. Chim. Acta 359 (2006) 883.
[8] M. Nonoyama, K. Suzuki, K. Yamasaki, Proc. Jpn. Acad. 45 (1969) 605.
[9] (a) M.I. Bruce, B.L. Goodall, F.G.A. Stone, J. Organomet. Chem. 60 (1973) 343; (b) J.M. Patrick, A.H. White, M.I. Bruce, M.J. Beatson, D.St.C. Black, G.B. Deacon, N.C. Thomas, J. Chem. Soc., Dalton Trans. (1983) 2121; (c) M.I. Bruce, M.J. Liddell, G.N. Pain, Inorg. Synth. 26 (1989) 171.
[10] Q.-F. Zhang, K.-M. Cheung, I.D. Williams, W.-H. Leung, Eur. J. Inorg. Chem. (2005) 4780.
[11] K. Hiraki, Y. Obayashi, Y. Oki, Bull. Chem. Soc. Jpn. 52 (1979) 1372.
[12] J. Matthes, S. Gründemann, A. Toner, Y. Guari, B. Donnadieu, J. Spandl, S. Sabot-Etienne, E. Clot, H.-H. Limbach, B. Chaudret, Organometallics 23 (2004) 1424.
[13] J.G. Małecki, M. Jaworska, R. Kruszynski, J. Kłak, Polyhedron 25 (2005) 3012.
[14] P. Reveco, W.R. Cherry, J. Medley, A. Garber, R.J. Gale, J. Selbin, Inorg. Chem. 25 (1986) 1842.
[15] R.A. Zelonka, M.C. Baird, Can. J. Chem. 50 (1972) 3063.
[16] M.K. Weibel, H.J. Bright, J. Biol. Chem. 246 (1971) 2734.
[17] C. Bourdillon, C. Demaille, J. Moiroux, J.-M. Savéant, J. Am. Chem. Soc. 115 (1993) 2.
[18] V.S. Soukharev, A.D. Ryabov, E. Csöregi, J. Organomet. Chem. 668 (2003) 75.
[19] Bruker AXS, SAINT Software Reference Manual, Madison WI, 1998.
[20] G.M. Sheldrick, SHELXTL (Version 6.10), Bruker AXS Inc., Madison, Wisconsin, USA, 2000.
[21] S. Fernandez, M. Pfeffer, V. Ritleng, C. Sirlin, Organometallics 18 (1999) 2390.
[22] M.J.S. Dewar, E.W.T. Warford, J. Chem. Soc. (1956) 3581.
[23] M.I. Bruce, Angew. Chem., Int. Ed. Engl. 16 (1977) 73.
[24] J. Dehand, M. Pfeffer, Coord. Chem. Rev. 18 (1976) 327.
[25] A.D. Ryabov, Chem. Rev. 90 (1990) 403.
[26] A. Albinati, C.G. Anklin, F. Ganazzoli, H. Ruegg, P.S. Pregosin, Inorg. Chem. 26 (1987) 503.
[27] C.G. Anklin, P.S. Pregosin, F.J. Wombacher, H. J Ruegg, Organometallics 9 (1990) 1953.
[28] A.B.V. Lever, Inorg. Chem. 29 (1990) 1271.
[29] A.J. Bard, L. R Faulkner, Electrochemical Method. Fundamentals and Applications, John Wiley & Sons, New York, 1980.